Two-color light-emitting-diode source for high-precision phase-shifting interferometry

L. Deck and F. Demarest

Zygo Corporation, Laurel Brook Road, Middlefield, Connecticut 06455-0448

We describe a two-color light-emitting-diode source that provides intense, uniform, and highly stable illumination with a wavelength precision sufficient for multiwavelength phase-shifting interferometry applications. The source has feedback-stabilized intensity and junction temperature sensing for wavelength compensation. It has a theoretical mean time between failure of more than 30,000 h, and the two colors provide a step measurement capability of greater than 2.5 μm. Measurements made with this source in an interferometric microscope show subangstrom repeatability.

Light-emitting diodes (LED's) have many appealing features as illumination sources for microscopy.[1] They have extremely high modulation bandwidths, well-defined spectra, long life, and low cost and are very small and generate little heat. With proper drive electronics, the illumination is exceptionally stable. In recent years, substantial improvements in LED luminosity, efficiency, and wavelength options have broadened their appeal and made them excellent alternatives to more conventional microscopy sources. In this Letter we present a novel two-color LED source specifically designed for use with multiwavelength phase-shifting interferometry (MWPSI) techniques. The source provides intense, stable illumination and is electronically switchable between two colors. A method for compensating for temperature dependencies of the wavelength is presented that keeps the mean wavelength uncertainty to less than 0.1 nm.

Phase-shifting interferometry is a common optical technique for noncontact surface profilometry[2,3] but requires the surface be smooth relative to the mean wavelength of the illumination. Surface discontinuities greater than a quarter wavelength cannot be unambiguously resolved with a single-wavelength measurement owing to the cyclic nature of the interference. Multiwavelength measurements extend this range by performing (at least) two phase measurements at different wavelengths.[4-6] The difference between these two phase measurements is identical to a single phase measurement performed at an equivalent wavelength given by $\lambda_{eq} = \lambda_1\lambda_2/|\lambda_1 - \lambda_2|$. The maximum resolvable discontinuity is then equal to a quarter of the equivalent wavelength. Unfortunately the single-wavelength measurement phase errors are scaled up by the ratio of λ_{eq} to the average wavelength of the two colors, which can impose severe constraints on wavelength accuracy and environmental stability.[7] Illumination sources for MWPSI must provide sufficiently stable illumination and wavelength accuracy to account for this scaling.

An illumination source designed to provide this capability is shown in Fig. 1. It consists of 60 LED's of two colors: 44 primary-color LED's with a mean wavelength of 650 nm and 16 secondary-color LED's with a mean wavelength of 613 nm. The spectral shape of both colors is approximately Gaussian with a FWHM of 25 nm, creating a temporal coherence length of approximately 8 μm FWHM. The equivalent wavelength of this combination is 10.77 μm, providing greater than 2.5 μm of unambiguous height resolution for discontinuous surface features.

The LED's are mounted such that their light cones overlap, producing an intense and highly uniform illuminated area that serves as the interferometer source plane. The LED's are electrically connected as shown in Fig. 2, providing independent control of the two colors. The parallel/series combination is a good compromise between electrical efficiency and reliability and tends to reduce the effect of small LED voltage drop variances that lead to inequities in current sharing. An aluminum cover is fastened over the exposed diode leads, producing a cavity into which a thermally conductive epoxy is poured to provide the leads with a good heat sink. The complete assembly is extremely rugged, weighs less than 225 g, and consumes less than 6 W of electrical power yet supplies as much as 50 mW of usable optical power. The LED's are rated at a mean time between failure of 2,000,000 h, making the source
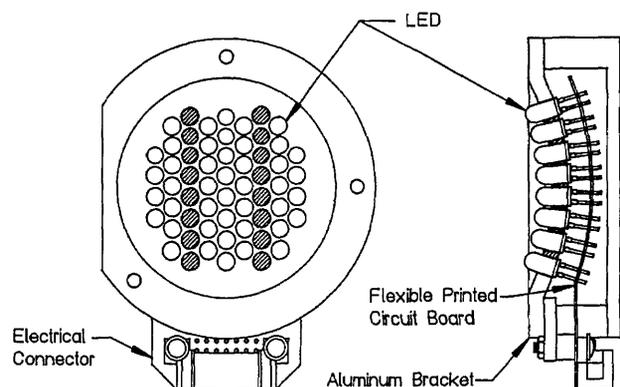

Fig. 1. Layout of the LED source assembly showing locations of the primary- and secondary-wavelength LED's.
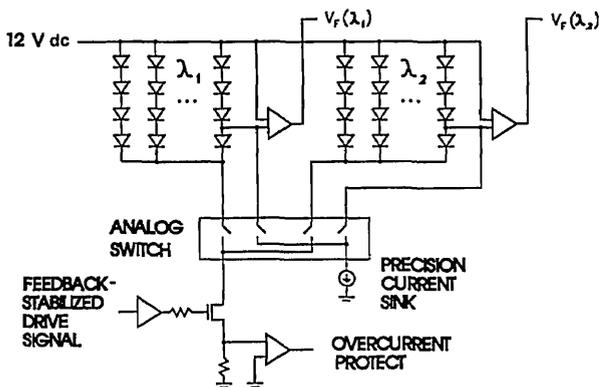
Fig. 2. Basic LED electrical schematic. $V_F(\lambda_{1,2})$ are the two points where the LED voltage drops are measured for temperature compensation. The analog switch controls which LED group is energized.

mean time between failure 33,000 h. A single LED failure reduces the source luminosity, depending on which series of four is effected, and provides the user with a warning that the source requires replacement while the instrument still functions.

Both the LED luminosity and mean wavelength are functions of junction temperature. The relationship between forward voltage (V_F) and forward current (I_F) for a forward-biased LED is

$$I_F = I_0 \exp\left(\frac{qV_F}{\alpha kT}\right), \qquad (1)$$

where I_0 is the saturation current, q is the electronic charge, T is the absolute temperature, k is Boltzmann's constant, and α is a temperature coefficient that is a function of temperature, I_F, and the type of recombination mechanism. Temperature-induced changes in forward current, and hence in optical power, are compensated for by a change in the forward current proportional to an error signal generated by a standard optical feedback loop. Unfortunately, as the junction temperature increases, the semiconductor band gap tends to decrease, increasing the mean wavelength. This variation, between 0.10 and 0.17 nm/°C for the LED's used, would require an accurate wavemeter to be compensated for directly. Instead we chose an indirect approach, that of measuring the junction temperature and applying a correction to the nominal wavelength derived from a precalibration of the source.

Equation (1) provides the basis for the direct measurement of the junction temperature. If we assume a constant temperature coefficient (α) and measuring V_F at constant I_F at two different temperatures, Eq. (1) gives

$$T_2 = \frac{T_1 V_F(T_2)}{V_F(T_1)}. \qquad (2)$$

Thus, once V_F is measured at a known temperature and current, the junction temperature can be deduced by another measurement of V_F at the same current. The assumptions used in deriving Eq. (2) mean that the temperature obtained may not be

accurate, but the method is still useful as a way of parameterizing the wavelength. A precision current sink, shown in Fig. 2, provides the constant forward current required for the temperature measurement. To minimize self-heating, we set the sink current to only 100 μA, and to reduce thermal decay we measure the voltage drop within 250 μs. The temperature measurement repeatability achieved was 0.1 °C rms.

Each source is calibrated separately with the following procedure. With the LED's off, the source is allowed to reach thermal equilibrium at 25 °C, the calibration temperature. The precision current sink momentarily supplies forward current, and V_F is sampled, held, and digitized. The current sink is then turned off, and the LED's are driven at a current setting high enough to provide sufficient light for a spectrophotometer measurement and again allowed to come to thermal equilibrium, which takes approximately 100 ms. The spectrum is measured, and another measurement of V_F is made with the current supplied by the precision current sink. This is repeated at intervals throughout the operating current range of the source. A table of temperature versus wavelength is then constructed utilizing Eq. (2) with the measured spectra and voltages. Figure 3 shows the results of three consecutive calibrations for each color for a typical source. The increased uncertainty seen at lower temperatures is an artifact of the reduced intensity produced at lower current settings, creating a poorer spectrum measurement. All the calibrations agree to within 0.1-nm rms for both colors. For uncorrelated uncertainties of 0.1-nm rms for each wavelength, the fractional error in the equivalent wavelength λ_{eq} is 0.4%.

The phase calculation in phase-shifting interferometry depends of the precise measurement of the intensity of the interferogram at specific points in time. Source intensity fluctuations contribute to errors in the phase calculation, and the extent of these errors is dependent on the frequency of the intensity fluctuations and the phase-shifting interferometry algorithm.[8,9] Figure 4 represents the measured intensity noise spectrum of the LED source compared with that from a filtered halogen bulb typically used in microscopes. The temporal noise of the LED source is at least 20 dB lower across the shown
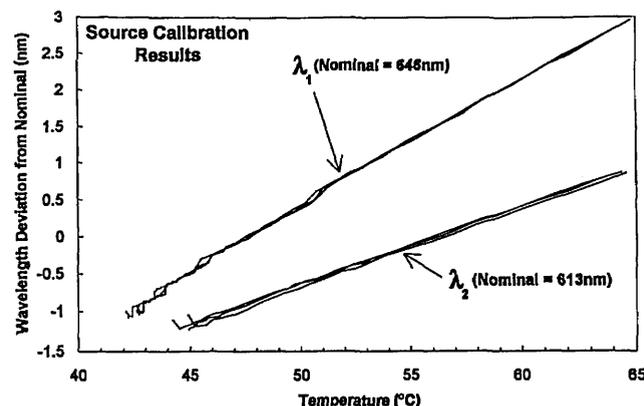

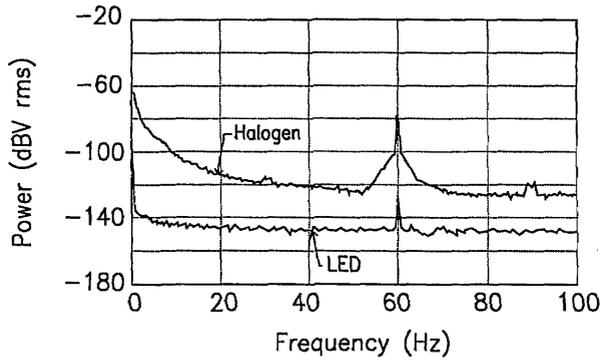Fig. 3. Results of repeated LED source calibrations for both wavelengths.

Fig. 4. Power spectrum of the intensity fluctuations of the LED source compared with that of a commercial microscope halogen lamp.
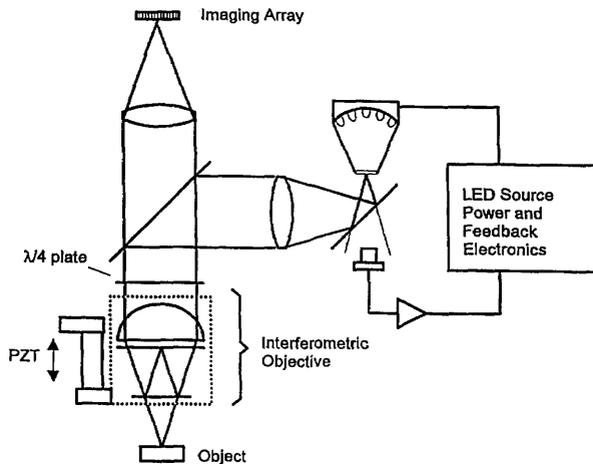

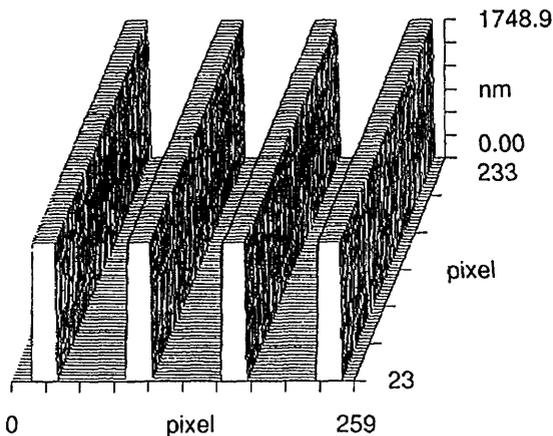Fig. 5. Schematic diagram of an optical profiler that uses the LED source.

Fig. 6. Measurement of a grating from a 1.75-μm step-height standard by multiwavelength phase-shifting interferometry with an optical profiler that uses the LED source. The average measured height was 1.74 μm.

spectrum. Of particular interest are frequencies below 60 Hz, which produce ripple in the profile that can seriously limit the resolution of the instrument. These frequencies are greatly suppressed in the LED source.

The layout of a profiler that uses this source is shown in Fig. 5. Light from the source is split by a

polarized beam splitter, and one component is used to provide the feedback for intensity stabilization through the monitor photodiode shown. The other component enters the instrument optical axis via another polarized beam splitter and is directed past a quarter-wave plate to an interferometric objective. The interferogram produced is then imaged onto an imaging sensor. Phase shifting is accomplished by moving the interferometric objective. After the test object is brought into focus and the measure cycle started, the instrument automatically adjusts the light level of the primary color while energizing the piezoelectric transducer (PZT). The primary-color phase measurement is then made. Temperature measurements are made immediately before and after the phase measurement. If a multiwavelength measurement was selected, the process is repeated with the secondary color. A MWPSI analysis follows, and the results are displayed. At no time during data taking is the operator required.

The automated nature of the measurement and the exceptional source temporal stability combine to provide extremely repeatable measurements. As a test of the measurement repeatability, the difference between two successive measurements of a smooth flat achieved a residual roughness of 0.09-nm rms. Figure 6 is a measurement of a grating from a 1.73-μm step-height standard and is a good example of a surface that requires MWPSI to be measured. The average measured step height was 1.740 μm, which agreed well with both the quoted step and a stylus result of 1.745 μm.

In conclusion, we have developed a solid-state two-color source whose temporal stability and wavelength accuracy make it ideal for interferometric profilometry. The source is small, intense, and extremely long lived and permits flexible, automatic control of intensity and wavelength. When used in MWPSI based profiler, the instrument achieves subangstrom vertical resolution with a single measurement.

References

1. T. Fujihara, Y. Shimada, C. Nagano, and K. Tsukamoto, "Illuminating device for microscopes," U.S. patent 4,852,985 (August 1, 1989).
2. J. C. Wyant, C. L. Koliopoulis, B. Bushan, and D. Basila, J. Tribol. **108**, 1 (1986).
3. J. F. Biegen and R. A. Smythe, Surf. Topography **1**, 469 (1988).
4. T. A. Nussmeier, "Interferometric distance measurement method," U.S. patent 4,355, 899 (October 26, 1982).
5. Y. Y. Cheng and J. C. Wyant, Appl. Opt. **23**, 4539 (1984).
6. K. Creath, Appl. Opt. **26**, 2810 (1987).
7. P. J. de Groot and S. Kishner, Appl. Opt. **30**, 4026 (1991).
8. C. P. Brophy, J. Opt. Soc. Am. A **7**, 537 (1990).
9. J. van Wingerden, H. J. Frankena, and C. Smorenburg, Appl. Opt. **30**, 2718 (1991).